THE EFFECTS OF SPATIAL RESOLUTION, SPECTRAL RESOLUTION, AND SIGNAL-TO-NOISE RATIO ON GEOLOGIC MAPPING USING HYPERSPECTRAL DATA, NORTHERN GRAPEVINE MOUNTAINS, NEVADA
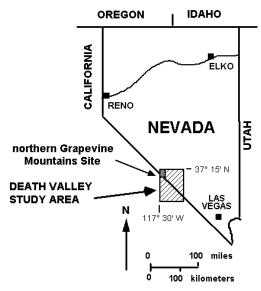
F. A. Kruse[*]

1.0 Introduction

A variety of multispectral and hyperspectral data have been collected for a site in the northern Grapevine Mountains, Nevada, spanning the period 1982 - 1999. Results described here are for both high and low altitude Airborne Visible/Infrared Imaging Spectrometer (AVIRIS) data, HyMap, and MODIS/ASTER Airborne Simulator (MASTER) data. These data have been analyzed separately, however, no detailed comparison of the information extracted from each dataset or the reasons for differences has previously been performed. This paper discusses the effects of the spatial resolution, spectral resolution, and signal-to-noise ratios of these data on geologic mapping at this site. Key findings are extrapolated to predict the effect of instrument characteristics and performance on geologic mapping using future satellite systems such as EO-1 Hyperion and ARIES.

2.0 Study Area

Figure 1: Location map

The northern Grapevine Mountains (NGM) site, located in south-central Nevada (Figure 1), consists of about one third of the "West of Gold Mountain" U.S. Geological Survey 7 1/2 minute quadrangle (1:24,000 scale). The site has been studied in detail using field mapping and several remote sensing data sets (Kruse, 1988, Kruse et al., 1993; Kruse et al., 1999a). Existing geologic maps include 1:62,500-scale bedrock mapping by (Wrucke et al. (1984) and mapping of surficial deposits by Moring (1986). More detailed site-specific mapping has also been performed (Kruse, 1988). PreCambrian bedrock in the NGM area consists of limestones, dolomites, sandstones and their contact metamorphic equivalents, however, published geologic maps do not distinguish between the different lithologies. Mesozoic plutonic rocks are mapped primarily as granitic-composition and some age-dates are available (Albers and Stewart, 1972). Mesozoic units mapped in the field as part of this research include quartz syenite, a quartz monzonite porphyry stock, quartz monzonite dikes, and a granite intrusion (Kruse, 1988). These rocks are cut by narrow north-trending mineralized shear zones containing sericite (fine grained muscovite or illite) and iron oxide minerals (Wrucke et al., 1984; Kruse, 1988). Slightly broader northwest-trending zones of disseminated quartz, pyrite, sericite, chalcopyrite, and fluorite mineralization (QSP alteration) ± goethite occur in the quartz monzonite porphyry. This type of alteration is spatially associated with fine-grained quartz monzonite dikes (Kruse, 1988). There are several small areas of quartz stockwork (silica flooding of the rocks) exposed at the surface in the center of the area, and skarn, composed mainly of brown andradite garnet near contact zones with limestone/dolomite. Complexly faulted, Tertiary volcanic rocks related to the Timber Mountain Caldera in southern Nevada are abundant around the southern periphery of the study area and are overlain by volcaniclastic sedimentary rocks interbedded with rhyolite and basalt (Wrucke et al., 1984). Quaternary deposits include Holocene and Pleistocene fanglomerates, pediment gravels, and alluvium.

3.0 Description of Data Used

Because the site was relatively well understood and mapped, repeated overflights of the NGM site with a variety of remote sensing instruments were arranged from 1982 through 1999 to evaluate remote sensing technology for resource assessment and to develop advanced analysis methodologies. Remote sensing data available for the NGM site include Landsat MSS and TM, Thermal Infrared Multispectral Scanner (TIMS), MODIS/ASTER (MODIS) Airborne Simulator, JPL Airborne Synthetic Aperture Radar (AIRSAR) and SIR-C. Imaging spectrometer

[*]Analytical Imaging and Geophysics, Boulder, CO 80303 (kruse@aigllc.com)

(hyperspectral) data flown for the NGM site include GER Spectral Profiler (1982), Airborne Imaging Spectrometer (AIS) (1984 - 1986), Airborne Visible/Infrared Imaging Spectrometer (AVIRIS) (1987, 1989, 1992, 1994, 1995), Low Altitude AVIRIS (1998), and HyMap (1999). Table 1 summarizes the characteristics of selected datasets and for the planned EO-1 and ARIES satellites.

Table 1: Data acquired and planned for the NGM site, 1982 - 2001

Instrument/Data	Date	Spatial Res.	No. Bands/Spectral Res	SWIR SNR
GER Profiler	1982	20 m	64/~8 nm	500:1
AIS	1984-1986	11-14 m	128/~9.3 nm	~20:1
AVIRIS	1987	20 m	224/~10 nm	15:1
AVIRIS	1989	20 m	224/~10 nm	50:1
AVIRIS	1992	20 m	224/~10 nm	100:1
AVIRIS	1994	20 m	224/~10 nm	100:1
AVIRIS	1995	20 m	224/~10 nm	400:1
AVIRIS	1998	2.4 m	224 (52 in range)/~10 nm	400:1
HyMap	1999	3.7 m	126 (29 in range)/~17 nm	>500:1+
MASTER	1999	4.3 m	50 (6 SWIR)/~50 – 70 nm	~450:1
EO-1 Hyperion	2000	30 m	220 (50 in range)/~10 nm	50:1
ARIES (planned)	2001+	30 m	~100 (32 SWIR)/~16nm	400:1

4.0 Spatial Resolution Comparisons: 1995 and 1998 AVIRIS

Direct comparison of the effects of spatial resolution on geologic mapping capabilities requires that the other variables, spectral resolution and SNR be held constant. The 1995 and 1998 AVIRIS data collections over the NGM site offer this opportunity, sharing approximately 10nm spectral resolution and SNR of approximately 400:1. Both datasets were corrected to apparent reflectance using ATREM (CSES, 1999). The 1995 data were acquired from the ER-2 platform, with an approximate 20m pixel. The AVIRIS sensor was flown over the NGM site on a twin Otter aircraft at low altitude during October 1998 as part of NASA/JPL's low altitude AVIRIS test project (Green et al., 1999a; Green et al., 1999b). The data were corrected to ~2.4 meter pixels (with some undersampling) using on board navigation and GPS (Boardman, 1999). Figure 2 shows a subset of the two datasets for comparison.
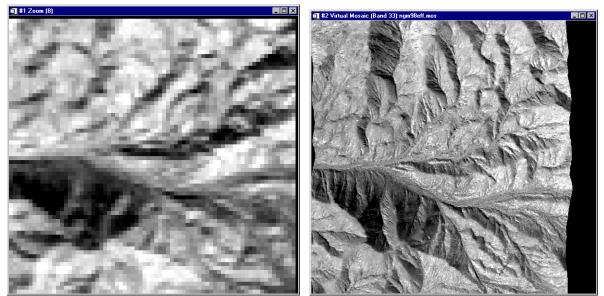

Figure 2: Comparison of 1995 (left, 20m) and 1998 (2.4m, right) AVIRIS data (band 31, 0.67 μm). Images are approximately 1.4 km across.

These AVIRIS subscenes show the general effect of resolution on the ability to visually recognize geologic features. As expected, the 20m data are much less clear, and more difficult to interpret. For example, the right image (2.4m pixels) shows clear evidence of faulting along the center, lower edge. This isn't at all apparent in the left image (20m pixels). Figure 3 shows the effect that the spatial resolution has on the spatial scale of spectral mapping and identification. Both images show gray-scale images for the mineral "sericite", mapped using Mixture-Tuned Matched Filtering (MTMF) (Boardman, 1998a). These images show subpixel occurrences greater than 10 percent for sericite, with brighter pixels representing higher concentrations. Note the general smoothing of the mineral map by the 20m AVIRIS data (left). Also note that some lower concentrations of sericite seen in the 2.4m data are absent in the 20m AVIRIS mineral map. Also less obvious in the 20m data is the NE trending mineralization seen along the right edge of the 2.4m data.
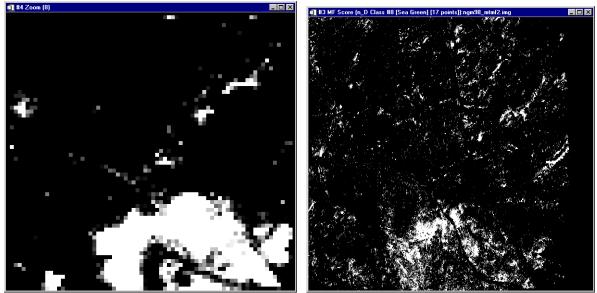

Figure 3: Comparison of 1995 (left, 20m) and 1998 (2.4m, right) AVIRIS MTMF results for "sericite" at the same threshold (abundances >10%). Images are approximately 1.4 km across.

5.0 SNR Comparisons: 1989, 1992, and 1995 AVIRIS

Direct comparison of the Signal-to-Noise-Ratio (SNR) of hyperspectral data requires holding the spatial and spectral resolution constant. This requirement is satisfied by examining AVIRIS data acquired over the period 1989 – 1995 on the ER-2 platform for the NGM site. These data share 20m spatial resolution and approximately 10nm spectral resolution. All data were corrected to apparent reflectance using ATREM (CSES, 1999). SNR for these datasets were not directly computed. Instead, reported SNR for the acquisition year SNR under standard AVIRIS radiance conditions (50% reflectance, solar noon) were used to select a range of representative data. Reported SNR for these data are approximately: 50:1 (1989), 100:1 (1992), and 400:1 (1995) for the D spectrometer (2.0 – 2.5 µm) as reported by Green et al., 1990; 1993, 1996. The 1995 data were also corrected for residual systematic errors utilizing the EFFORT method of Boardman (1998b). This correction is only possible on the 1995 data because of its exceptional signal-to-noise characteristics. Single-pixel spectra were extracted from the data for two key materials at the NGM site; carbonates, and sericitic alteration. Figure 4 shows spectral plots of the 1989, 1992, and 1995 reflectance spectra for calcite and dolomite endmembers. Though there are obvious SNR differences, the position of the diagnostic spectral feature for dolomite near 2.32 mm could be separated from the spectral feature for calcite at all SNR levels. It should be clear, however, that any automated feature-based method will have difficulty picking out the specific absorption features at the lower SNR levels. Figure 5 shows a comparison of spectral plots for single-pixels for sericitic alteration identified at the NGM site. First, note that for both the 1989 and 1992 cases, only two different sericite varieties were distinguishable. The 1995 data indicate that there are actually three distinct species of sericite at the NGM site based on the position of the main feature near 2.2 µm, a fact verified by microprobe analysis (Kruse et al., 1999a). Figure 6 demonstrates the effect of SNR on the spatial distribution derived from spectral mapping. At the 50:1 SNR, there is some calcite/dolomite confusion, and only the two sericites are mapped. At the 400:1 SNR, the calcite/dolomite mapping is improved, all three sericites can be mapped, and there is improved sub-pixel detection and abundance mapping.
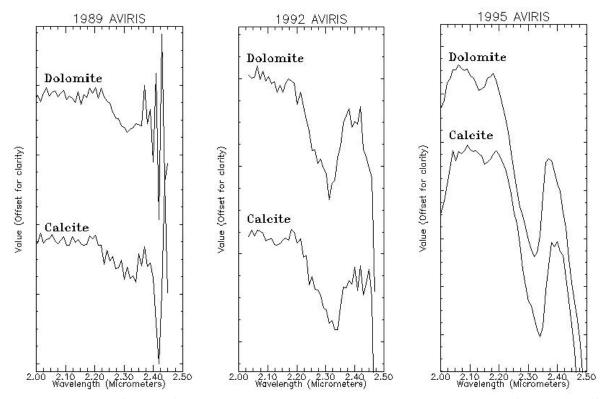
Figure 4 Comparison of 1989 (left), 1992 (center), and 1995 (right) single-pixel AVIRIS spectra for areas identified as calcite and dolomite at the NGM site.
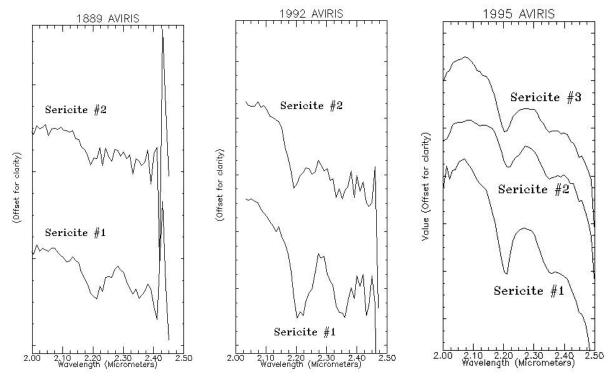

Figure 5 Comparison of 1989 (left), 1992 (center), and 1995 (right) single-pixel AVIRIS spectra for sericitic alteration at the NGM site.
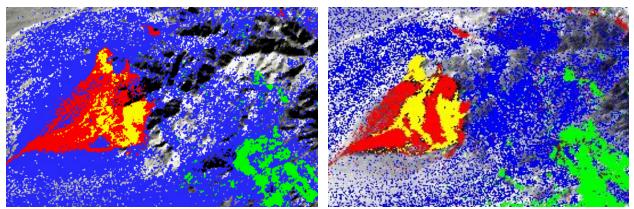
Figure 6 Comparison of 1989 (Spectral Angle Mapper results, left), and 1995 (MTMF results, right) AVIRIS mineral maps for carbonates and sericitic alteration at the NGM site. Printed as grayscale images, dolomite is white, forming the donut-shaped area in the center of the images; calcite is medium-gray, filling the center of the donut and surrounding areas; sericite #1 is the light gray area in the lower right hand portion of each image; sericite #2 is the dark gray area in both images, and sericite #3 is the small black area near the lower right corner of the right image. For color, yellow=dolomite, red=calcite, green=sericite#1, blue=sericite#2, brown=sericite#3 (right image only).

6.0 Spectral Resolution Comparisons: 1998 AVIRIS, 1999 HyMap, and 1999 MASTER

The 1998 low altitude AVIRIS, 1999 HyMap, and 1999 MASTER data offer the opportunity to compare the effect of spectral resolution on spectral signatures of the minerals at the NGM site. While not identical, these data do have similar (high) spatial resolutions (2.4m, 3.7m, 4.3m for AVIRIS, HyMap, and MASTER respectively) and similar (high) SNR ratios (400:1. >500:1, and ~450:1 for AVIRIS, HyMap, and MASTER respectively). Both AVIRIS and HyMap are hyperspectral sensors and the data were corrected to apparent reflectance using ATREM (CSES, 1999). AVIRIS has 32 bands in the 2.0 - 2.5 µm SWIR range with approximately 10 nm spectral resolution (Table 1) (Green et al., 1999b). HyMap is a state-of-the-art aircraft-mounted commercial hyperspectral sensor developed by Integrated Spectronics, Sydney, Australia, and operated by HyVista Corporation, Sydney, Australia (Cocks et al., 1998; Kruse et al., 1999b). HyMap has slightly broader spectral bands than AVIRIS at approximately 17 nm in the SWIR. The last 29 bands 2.0 – 2.48 µm) were used for this analysis. MASTER is an airborne simulator with 50 spectral bands, operated by NASA Ames Research Center in support of validation and scientific investigations utilizing MODIS and ASTER on the NASA Terra satellite (Simon Hook, Unpublished Data, 2000). Six spectral bands covering the 2.0 – 2.33 µm range with ~50-70 nm spectral resolution were used in this study. The data were corrected to apparent reflectance using an empirical line correction based on the 1999 HyMap ATREM apparent reflectance data. Figure 7 shows the spectral response of MASTER over this spectral range (the 2.39 mm band was excluded).
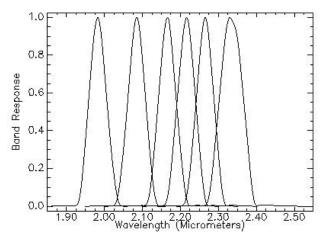

Figure 7 MASTER spectral bands 2.0 – 2.4 µm.

Figure 8 is a comparison of spectral plots for carbonates and sericites at the NGM site. Despite the fact that the HyMap spectral resolution (~17 nm) is nearly half that of the AVIRIS data (~10 nm), both sensors can successfully separate calcite from dolomite and all three varieties of sericite at the NGM site. The MASTER data, with only 6 spectral bands, and a much broader spectral resolution can separate carbonates from sericite, but can not separate either calcite from dolomite or differentiate the three sericites without *a priori* knowledge. Examination of known areas of calcite and dolomite does seem to indicate, however, that these minerals could be separated at the NGM site given a supervised classification utilizing known training sites. This is consistent with observed capabilities of other MASTER data (Simon Hook, Personal Communication, 2000).
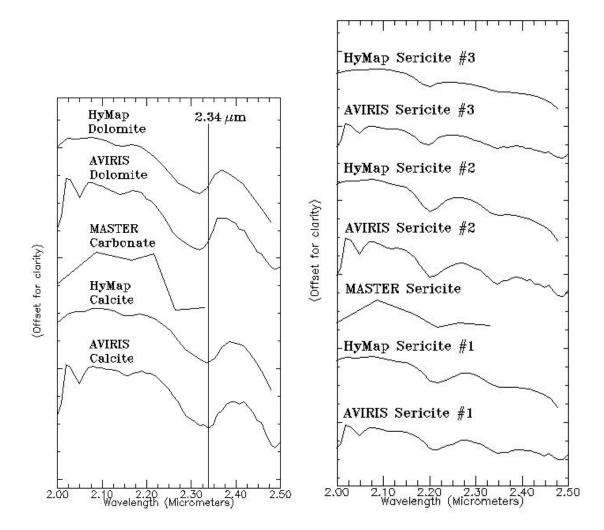

Figure 8: Comparison of 1998 low-altitude AVIRIS, 1999 HyMap, and 1999 MASTER spectra for selected endmembers.

The effect of spectral resolution on spatial mineral mapping is shown in Figure 9. The HyMap data show the clear separation of the three varieties of sericite. The MASTER image shows how the three different sericites are grouped as one material because of the fact that the spectral resolution is inadequate to resolve the small shifts in the position of the main spectral feature at 2.2 μm.
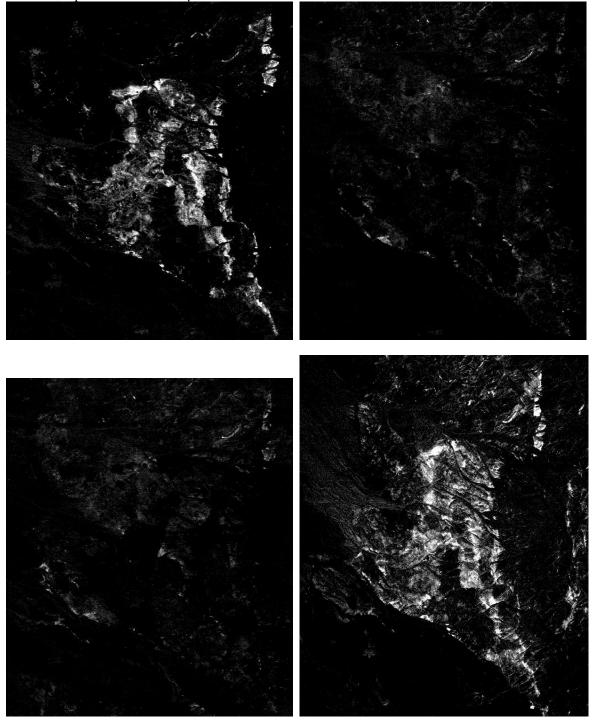

Figure 9: Comparison of "sericite" endmember mapping (MTMF) for 1999 HyMap and 1999 MASTER data.
        Upper left: HyMap Sericite #1, Upper Right: HyMap Sericite #2, Lower Left: HyMap Sericite #3, Lower
        right: MASTER Sericite. Images are approximately 2.6 km across. Brighter pixels represent higher
        abundances.

7.0 Conclusions

The results above demonstrate that spatial resolution, spectral resolution, and SNR have dramatic effects on the ability to perform mineral mapping using hyperspectral data. Spatial resolution is the key to mapping of detailed, scale-dependent variation. Increasing the pixel size (decreasing the spatial resolution) results in the loss of image detail. There is a tendency to lose small, discrete occurrences of specific materials with larger pixels. Spectral resolution is the key to separation of subtle material differences. Decreasing the spectral resolution results in losses in the ability to distinguish and map fine spectral detail. While not particularly apparent at this site because there are not any extremely fine spectral differences, coarser spectral resolution can prohibit discrimination and identification of specific minerals (cf: crystalline vs poorly-crystalline kaolinite at Cuprite, Nevada; Swayze, 1997). SNR is the key to overall quality of the spectral mapping process. There is decreased capability to define key spectra with decreasing SNR. If the SNR level is inadequate, neither spatial or spectral resolution matters.

Some final comments on expectations for EO-1 Hyperion and future satellite systems: We are NOT expecting Hyperion to perform like 1999 AVIRIS! Hyperion will, however, demonstrate the viability of Satellite Hyperspectral Sensing. A key factor is its potential for site acquisition world-wide. We expect that Hyperion will be useful for geologic mapping on about the level of the 1989 AVIRIS data. Its 30m spatial resolution, 10 nm spectral resolution, and SWIR SNR of 50:1 should produce results similar to those shown for the 1989 AVIRIS data in Figures 4, 5, and 6. These capabilities will be combined with airborne systems such as AVIRIS and HyMap to allow scaling of higher spatial and spectral resolution measurements. Future satellite systems should provide sufficient spatial resolution to allow overview coverage (trade off for SNR), spectral resolution around 10 - 20 nm (trade off for SNR), and SNR "as high as possible".

9.0 References Cited

Albers, J. P., and Stewart, J. H., 1972, Geology and mineral deposits of Esmeralda County, Nevada: Nevada Bureau of Mines and Geology Bulletin 78, 80 p.

Boardman, J. W., 1998a, Leveraging the high dimensionality of AVIRIS data for improved sub-pixel target unmixing and rejection of false positives: mixure tuned matched filtering, in: Summaries of the Seventh Annual JPL Airborne Geoscience Workshop, Pasadena, CA, p. 55.

Boardman, J. W., 1998b, Post-ATREM polishing of AVIRIS apparent reflectance data using EFFORT: a lesson in accuracy versus precision: in Proceedings of the 8th JPL Airborne Earth Science Workshop: Jet Propulsion Laboratory Publication 99-17, p. 53.

Boardman, J. W., 1999, Precision geocoding of AVIRIS low-altitude data: lessons learned in 1998: in Proceedings of the 8th JPL Airborne Earth Science Workshop: Jet Propulsion Laboratory Publication 99-17, p. 63 – 68.

Cocks T., R. Jenssen, A. Stewart, I. Wilson, and T. Shields, 1998, The HyMap Airborne Hyperspectral Sensor: The System, Calibration and Performance. *Proc. 1st EARSeL Workshop on Imaging Spectroscopy* (M. Schaepman, D. Schläpfer, and K.I. Itten, Eds.), 6-8 October 1998, Zurich, EARSeL, Paris, p. 37-43.

Center for the Study of Earth from Space (CSES), 1999, Atmosphere REMoval Program (ATREM) User's Guide, Version 3.1, Center for the Study of Earth from Space, Boulder, Colorado, 31 p.

Green, R. O., Conel, J. E., Carrere, V., Bruegge, C. J., Margolis, J. S., Rast, M., and Hoover, G., 1990, Determination of the in flight spectral and radiometric characteristics of the Airborne Visible/Infrared

Imaging Spectrometer (AVIRIS): in Proceedings, 2nd Airborne Visible/Infrared Imaging Spectrometer (AVIRIS) workshop, JPL Publication 90-54, p. 15 - 34.

Green, R. O., Conel, J. E., Helmlinger, M., van den Bosch, J., Chovit, C. and Chrien, T., 1993, Inflight calibration of AVIRIS in 1992 and 1993: in Summaries, 4th Annual JPL Airborne Geoscience Workshop, JPL Publication 93-26, p. 69 - 72.

Green, R. O., Conel, J. E., Margolis, J., Chovit, C., and Faust, J., 1996, In flight calibration and validation of the Airborne Visible/Infrared Imaging Spectrometer (AVIRIS): in Proceedings, 6th Airborne Visible/Infrared Imaging Spectrometer (AVIRIS) workshop, JPL Publication 96-4, v. 1, p. 115 - 126.

Green, R. O., Chrien, T. G, Sarture, C., Eastwood, M, Chippendale, B., Kurzweil, C., Chovit, C., and Faust, J. A., 1999a, Operation, calibration, georectification, and reflectance inversion of NASA's Airborne Visible/Infrared Imaging Spectrometer (AVIRIS) four- and two-meter data acquired from a low-altitude platform: in Proceedings of the 8th JPL Airborne Earth Science Workshop: Jet Propulsion Laboratory Publication 99-17, p. 177 – 188.

Green, R. O., Pavri, B., Faust, J., Chovit, C., and Williams, O., 1999b, AVIRIS in-flight radiometric calibration results for 1998: in Proceedings of the 8th JPL Airborne Earth Science Workshop: Jet Propulsion Laboratory Publication 99-17, p. 161 – 176.

Kruse, F. A., 1988, Use of Airborne Imaging Spectrometer data to map minerals associated with hydrothermally altered rocks in the northern Grapevine Mountains, Nevada and California: Remote Sensing of Environment, v. 24, no. 1, pp. 31-51.

Kruse, F. A., Lefkoff, A. B., and Dietz, J. B., 1993a, Expert System-Based Mineral Mapping in northern Death Valley, California/Nevada using the Airborne Visible/Infrared Imaging Spectrometer (AVIRIS): Remote Sensing of Environment, Special issue on AVIRIS, May-June 1993, v. 44, p. 309 - 336.

Kruse, F. A., Boardman, J. W., and Huntington, J. F., 1999a, Fifteen Years of Hyperspectral Data: northern Grapevine Mountains, Nevada: in Proceedings of the 8th JPL Airborne Earth Science Workshop: Jet Propulsion Laboratory Publication, JPL Publication 99-17, p. 247 - 258.

Kruse, F. A., Boardman, J. W., Lefkoff, A. B., Young, J. M., Kierein-Young, K. S., and Cocks, T., 1999b. The 1999 USA HyMap Group Shoot: In Proceedings, ISSSR'99, 31 October – 4 November 1999, Las Vegas, Nevada (In Press)

Moring, B., 1986, Reconnaissance surficial geologic map of northern Death Valley, California and Nevada: U. S. Geological Survey Miscellaneous Field Studies Map MF-1770, 1:62,500, 1 sheet.

Swayze, G. A. 1997, The hydrothermal and structural history of the Cuprite Mining District, Southwestern Nevada: An integrated geological and geophysical approach: Unpublished Ph. D Thesis, University of Colorado, Boulder, 341 p.

Wrucke, C. T., Werschkey, R. S., Raines, G. L., Blakely, R. J., Hoover, D. B, and Miller, M. S., 1984, Mineral resources and mineral resource potential of the Little Sand Spring Wilderness Study Area, Inyo County, California: U. S. Geological Survey Open File Report 84-557, 20 p.